



## 2 Operators and lattice techniques

In the  $0^{++}, 2^{++}$ -channel we consider gauge-invariant operators of various types, such as ones containing only scalar fields,  $R = \text{Tr}(\sum_x \phi_x \phi_x^\dagger)$ , scalar fields and links,  $L = \text{Tr}(\sum_x U_x \phi_x \phi_{x+\hat{\mu}}^\dagger)$ , and plaquettes  $P = \text{Tr}(U_p)$  consisting of gauge degrees of freedom only. In the  $1^-$  channel we know only one gauge-invariant operator,  $V^a = \text{Tr}(\sum_x \phi_x^a U_x \phi_{x+\hat{\mu}}^\dagger)$ . Another operator useful to clarify the properties of the regions in parameter space is the Polyakov loop operator,  $P_L(i) = \text{Tr} \prod_{x_i=1}^L U_{i(x+\hat{n})}$ , whose expectation value vanishes in a confining theory. In the Higgs model one expects this never to be the case as the string between fundamental charges eventually breaks beyond some large separation due to matter pair creation. In some of our simulations in the symmetric phase, however, the measured VEV's are statistically compatible with zero. This means that screening of the flux has not yet set in for separations as large as the spatial lattice size, and up to this distance the Wilson loop still behaves according to the area law. In these cases one may extract a volume-corrected string tension from the correlations of Polyakov loops according to<sup>4</sup>

$$a^2 \sigma = a^2 \sigma_L + \frac{1}{6L^2}; \quad aM_{PL}(L) = a^2 \sigma_L L; \quad (2)$$

where  $L$  is the spatial length of the lattice.

In order to improve the projection properties of our operators we "smear" the fields by covariantly connecting them with their neighbours<sup>2</sup>. The excitation spectrum may be computed by considering  $N$  operators  $\phi_i$  of different types and smearing levels for each quantum number and measure correlations between all of them. This correlation matrix can then be diagonalised numerically<sup>2</sup> resulting in a set of  $N$  (approximate) mass eigenstates of the Hamiltonian  $\hat{H} = \sum_{k=1}^N a_{ik} \phi_k$ , which are superpositions of the operators  $\phi_i$  used in the simulation. The coefficients  $a_{ik}$  are useful in identifying the contributions of the individual operators  $\phi_i$  to the mass eigenstates.

## 3 The spectrum at small and large scalar coupling

The mass spectrum at small scalar coupling  $g_3^2 = 0.0239$  is shown in Fig. 1 (a). In the Higgs phase there are the familiar Higgs and W bosons with a large gap to higher excitations representing scattering states with relative momentum. In the symmetric phase, on the other hand, there is a dense spectrum of bound states. Their composition may be characterised by considering the contributions  $a_{ik}$  of the individual operators to each eigenstate, Fig. 1 (b). The pure gauge plaquette operators,  $P$ , contribute very little to the ground state and the first excited state. However, the third  $0^{++}$  state is composed almost entirely of them. This suggests interpreting it as a "W-ball", in analogy to the

glueballs of pure gauge theory. In the Higgs phase the plaquette projects onto a two- $W$  scattering state, in agreement with perturbation theory.  $W$ -balls are also observed in the  $2^{++}$ -channel. The  $W$ -ball masses agree at the percent level with their pure gauge analogues<sup>4</sup>, indicating a fairly complete decoupling of the pure gauge sector. In Table 1 some properties of the Polyakov loop are

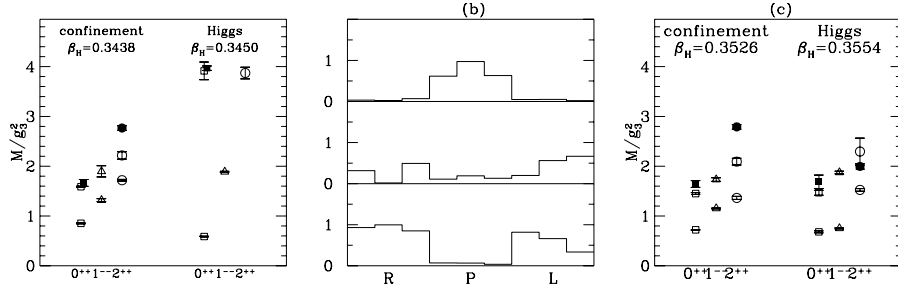


Figure 1: The lowest states of the spectrum in the confinement (left) and Higgs (right) regions for (a)  $g_3^2 = 0.0239$ , (c)  $g_3^2 = 0.274$ . Full symbols denote pure gauge states. (b) Coefficients  $a_{ik}$  of the  $0^{++}$  states on the confinement side of (a),  $i = 2$  for  $R; P; L; g$ .

listed. In the confinement phase its VEV is compatible with zero and one may extract a string tension which is about 97% of the one of pure gauge theory<sup>4</sup>. On the Higgs side it has a large VEV and no string tension exists. Instead, a perturbative expansion of the correlator is possible whose leading term corresponds to a two- $W$  state. Indeed, we find the effective mass of the Polyakov loop correlator to be compatible with twice the  $W$ -mass.

	conf.	Higgs
$\langle P \rangle_L$	0.001 (1)	6.535 (6)
$aM_{P,L}$	0.577 (8)	1.8 (1)
$aM_W$	0.610 (4)	0.836 (3)
$aP_W$	0.1582 (6)	{

Table 1: Properties of the Polyakov loop,  $g_3^2 = 0.0239$ .

Now consider the large scalar coupling  $g_3^2 = 0.274$ , where there is no phase transition anymore separating the two regions. The spectrum for this case is displayed in Fig. 1 (c). On the confinement side it qualitatively looks the same as before. We even find the masses of the  $W$ -ball states to be numerically compatible with those of the small scalar coupling case. This confirms the decoupling of the pure gauge sector over a range of scalar couplings of an

order of magnitude! On the Higgs side, a dramatic change has taken place, with the spectrum now qualitatively resembling that on the confinement side. Accordingly, perturbation theory is not applicable and one cannot identify the effective mass of the Polyakov loop with a two-W state. Does the confinement dynamics now extend to the other side of the crossover? Considering again the Polyakov loop, Fig. 2 (a), we see that this is not the case. Whereas the usual "order parameter"  $\langle R \rangle$  used to distinguish the phases only grows about 30 % from the confinement point to the Higgs point, the VEV of the Polyakov loop shows a pronounced increase. Despite the smoothness of the crossover a critical coupling  $\beta_H^c$  may be defined by the peak in the susceptibility of  $R$ ,  $\chi[R] = \langle R^2 \rangle - \langle R \rangle^2$ , which separates the Higgs and confinement regions, Fig. 2 (b). On the confinement side the effective mass of the Polyakov loop increases linearly with the lattice size as required to interpret it as a flux loop. On the Higgs side the VEV is large and no flux loops exist. We are thus led to conclude that the latter corresponds to a Higgs regime with strong scalar coupling.

#### 4 Continuous connection of the spectrum and flux loop decay

The four lowest  $0^{++}$ -states are connected through the crossover as shown in Fig. 2 (c). Note that the ground state dips but stays finite in accordance with the absence of a diverging correlation length in a crossover. In contrast, the mass of the W-ball is independent of  $\beta_H$  until beyond the critical coupling, which is yet another manifestation of its decoupling.

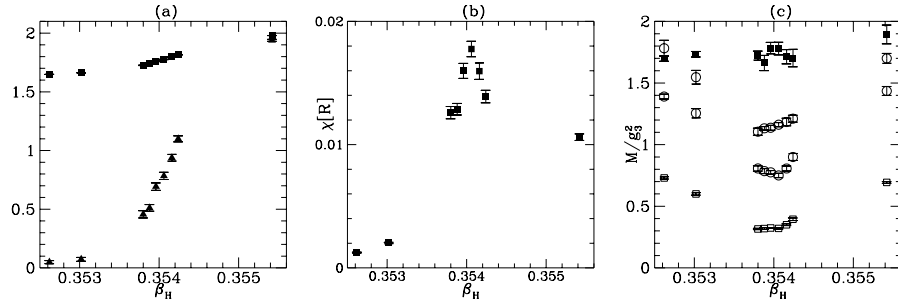


Figure 2: (a) Squares:  $\langle R \rangle$ , triangles:  $\langle P \rangle$ . (b) The susceptibility  $\chi[R] = \langle R^2 \rangle - \langle R \rangle^2$ . (c) The  $0^{++}$  states through the crossover. Full symbols denote the pure gauge state.

In Fig. 3 (a) the coefficients of the different operator types in the  $0^{++}$  ground state are shown. Throughout the crossover the dominating contribution comes from scalar operators. However, moving towards the critical point, there is an increasing contribution from plaquettes and Polyakov loops which

decreases again on the Higgs side. Due to decoupling, the converse is not true for the  $W$ -ball, Fig. 3 (b). The growing overlap of the Polyakov loop with the scalar ground state has a physical interpretation. Recall that the Polyakov loop projects on a flux loop in the confinement phase which does not exist on the Higgs side. The overlap with scalar states signals an increasing coupling between the flux loop and these states. A natural physical picture then is that the flux loop becomes increasingly unstable and eventually decays, where the  $0^{++}$  eigenstates are some of the possible decay products. Consequently the pole in the PL correlator moves away from the real axis. Its real part is given by the weighted sum of the energies of the decay products, the imaginary part by its decay width. To test this picture we define the "effective flux loop energy"  $E_F$  and the corresponding "decay width"  $\Gamma_F$  by

$$E_F \equiv \frac{\sum_i \langle j_{AP,L,i} | \hat{J}_M | i \rangle}{\sum_i \langle j_{AP,L,i} | \hat{J}^2 | i \rangle}; \quad \Gamma_F^2 = \langle E_F^2 \rangle - \langle E_F \rangle^2; \quad (3)$$

Numerical results for these are shown in Fig. 3 (c). The decay width is close to zero on the confinement side where flux loops are stable, and then increases towards the critical coupling maintaining a high value on the Higgs side. We conclude that the picture of a decaying flux loop is qualitatively confirmed.

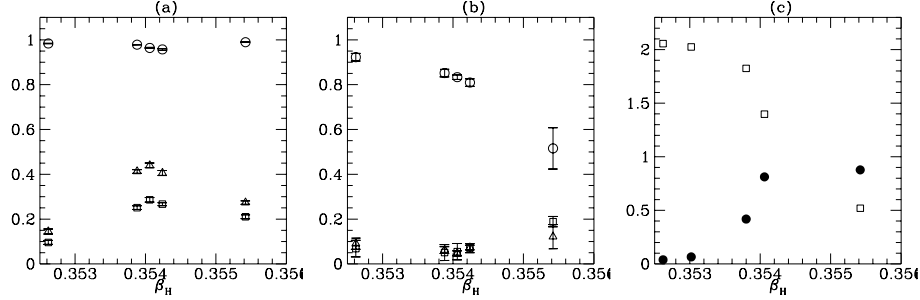


Figure 3: The  $a_{ik}$  of the (a)  $0^{++}$  ground state and (b) the  $0^{++}$   $W$ -ball. Circles denote  $R=L$  operators, squares  $P$  and triangles  $PL$ . (c) Squares:  $E_F$ , full circles:  $\Gamma_F$ .

## References

1. K. Kajantie, M. Laine, K. Rummukainen and M. Shaposhnikov, Phys. Rev. Lett. 77 (1996) 2887; M. Laine, these proceedings.
2. O. Philipsen, M. Teper and H. Wittig, Nucl. Phys. B 469 (1996) 445; Nucl. Phys. Proc. Suppl. 53 (1997) 626; HD-THP 97-37.
3. W. Buchmüller, these proceedings.
4. M. Teper, Phys. Lett. B 311 (1993) 223; P. de Forcrand G. Schierholz, H. Schneider and M. Teper, Phys. Lett. 160B (1985) 137.